

# Mobile Robot Localization Based On Low-Cost LTE And Odometry In GPS-Denied Outdoor Environment

Khairuldanial Ismail<sup>1</sup>, Ran Liu<sup>1</sup>, Jie Zheng<sup>2</sup>, Chau Yuen<sup>1</sup>, Yong Liang Guan<sup>3</sup> and U-Xuan Tan<sup>1</sup>

<sup>1</sup>*Pillar of Engineering Product Development*

*Singapore University of Technology and Design, Singapore*

<sup>1</sup>khairuldanial@mymail.sutd.edu.sg, <sup>1</sup>{ran\_liu, yuenchau, uxuan\_tan}@sutd.edu.sg

<sup>2</sup>*School of Information Engineering*

*Southwest University of Science and Technology, Sichuan, China*

<sup>2</sup>happenjz@163.com

<sup>3</sup>*School of Electrical and Electronics Engineering*

*Nanyang Technological University, Singapore*

<sup>3</sup>eylguan@ntu.edu.sg

**Abstract**—GPS localization has always been the go-to method for localizing mobile robots in outdoor environments. However, in GPS denied environments such as urban canyons, LTE becomes a better alternative. LTE localization exploits existing infrastructures and transmitted signals to provide an estimated position of the robot. As a low-cost solution, it benefits robots under the constraint of cost, size and weight. This paper proposes a particle filter based localization method by using only LTE and wheel odometry for GPS-denied outdoor environments. We used the fingerprinting method by obtaining LTE Cell ID, mean RSS and GPS location and associating these data to the grids in an initialized map. We resolved the position of the robot using recursive Bayesian estimation and particle filter for its implementation. In our experiment, we used a mobile robot and five smartphones to obtain the wheel odometry and LTE data respectively while travelling along a particular route in an outdoor environment. The method was able to obtain accurate localization results with RMSE of 13.07m. We further evaluated the parameters of the method effects on the localization accuracy achieved.

**Index Terms**—localisation, GPS denied, outdoor environment, particle filter, mobile robot

## I. INTRODUCTION

Localization is key to the autonomous capabilities of mobile robots as it enables mobile robots to navigate and maneuver through the environment on its own. However, as these mobile robots are becoming prevalent in the world, they are being subjected to unpredictable conditions of the environment which proves to be a challenge for localization. Outdoor environments, especially, are often difficult for these robots to effectively perform localization due to the weather, terrain and lighting conditions which adversely affects the quality of sensor data [1]. Researchers have introduced multi sensor fusion [2] [3] and Simultaneous Localization and Mapping (SLAM) algorithms [4] [5] to overcome such problems. While they do provide better quality of localization under such conditions, it comes with an increase cost to produce such

systems due to the cost of integrating many sensors and the expensiveness of a good quality sensor.

Outdoor environments often call for the use of Global Positioning System (GPS) since its readily available and designed for localization. The GPS receiver is required to receive signals from at least 4 satellites to determine its position. This in turn requires a clear line of sight between the receiver and the satellites. However, in environments such as urban canyons or tree canopy covers, buildings and trees become obstructions between the GPS receiver and the satellite [6]. In places where there are tall buildings, satellite signals would be reflected off its surface causing multipath effect on the GPS signal [9]. Hence, in such situations, GPS as a method of localization would perform poorly and the use of Signal of Opportunity (SOP), such as Long-Term Evolution (LTE), would be a better alternative. SOPs are signals that are already in transmission throughout the environment such as radio and mobile phone signals and hence, are readily available. However, even when SOPs are not designed for localization, researchers have proposed localization algorithms to capitalize on these signals [7] [8].

This paper proposes a particle filter (PF) based localization method for mobile robots to be able to localize in GPS denied outdoor environments with a low-cost sensor system involving LTE receivers and wheel encoders. The method proposed in this paper can be explained in two different phases as shown in figure 1. The first phase of the method is building the fingerprint map. The second phase of the method is implementing the localization method of either the KNN-based localization by obtaining position from LTE data measured against the prior fingerprint map or the PF-based localization to fuse wheel odometry from a mobile robot and position obtained from KNN-based localization. Our proposed PF-based localization gives an improved position estimate over wheel odometry by 82.60% and KNN-based localization by

62.87%.

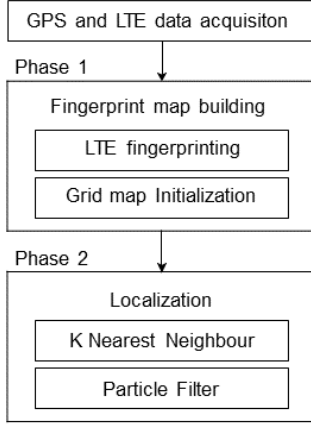


Fig. 1. This figure shows the overall process of the method proposed.

We organise the paper as follows. In Section II, we introduce prior related works that have been published. In Section III the paper explains the map-building phase of the method. In Section IV, the paper explains localization phase and the two methods for localization namely KNN-based localization and PF-based localization. In Section V, the paper describes the experiment that was done using the method proposed and presents the results as well as the evaluation on the parameters of the method for its effects on the localization accuracy. The paper will conclude in section VI.

## II. RELATED WORKS

Research in LTE localization have been an ongoing interest in the past decade. With the objective to improve localization accuracy, many solutions such as SLAM and machine learning algorithms have been explored and proposed. In [10], the research proposes a method called signalSLAM which combines Radio Frequency (RF) signals such as WiFi, 4G LTE or Bluetooth from multiple sources and pose from Pedestrian Dead Reckoning (PDR) obtained from a smartphone to build a fingerprint map for localization. This method also mentions that users can contribute to a crowdsourced map while doing their daily activities. It then uses modified GraphSLAM to estimate the pose of users based on the similarity between absolute location and constraints. [11] proposes a neural network assisted localization using LTE fingerprints. It has a feature extraction algorithm for obtaining relevant fingerprints for the training phase. In the localization phase, a feedforward neural network learn based on these fingerprints and locations to obtain a model for estimating the pose of the user's equipment (UE). [12] proposes a similar method where the LTE fingerprint map was obtained for the training phase but the localization had a two layer implementation. The first layer uses Weighted K-Nearest Neighbors (WKNN) to reduce the complexity of training its neural network which forms the second layer by filtering the relevant fingerprints for localization. The trained model is then used to estimate

the pose of the UE. All these methods utilize fingerprints for localization and they managed to perform localization at low-cost. However, most methods to the best of our knowledge, including the three methods described, do not apply LTE localization to mobile robotics. Mobile robots allow the use of multiple sensors for localization outdoors but at the constraint of its cost, size and weight. Hence, through enabling LTE localization for mobile robots, the method proposed in this paper aims at introducing a low-cost and accurate alternative to performing outdoor localization especially for robots that are conditioned by these design constraints.

## III. MAP-BUILDING

### A. LTE Fingerprinting

In order to use LTE for localization, LTE data must be mapped to geographical locations. We achieve that by obtaining pairwise data of geographical locations and its corresponding LTE data. The LTE data that we considered for this method involves the combination of Physical Cell Identity (PCI) and E-UTRA Absolute Radio Frequency Channel Number (EARFCN) which forms a Cell ID along with its respective mean Received Signal Strength (RSS). PCI identifies the physical device while EARFCN distinctively identifies the LTE band and carrier frequency. Hence, cell ID varies amongst the different cellular network providers and base transceiver stations. However, Cell ID is unique over a certain distance. GPS was used to obtain geographical location based on World Geodetic System 84 (WGS84) in longitude and latitude. The accumulation of the pairwise data forms a fingerprint vector as shown in equation 1.

$$\mathbf{F} = \{(\mathbf{f}_1, \mathbf{g}_1), \dots, (\mathbf{f}_M, \mathbf{g}_M)\} \quad (1)$$

for a fingerprint vector  $\mathbf{F}$  with  $M$  fingerprints where  $\mathbf{f}_i$  is the LTE data associated with GPS location  $\mathbf{g}_i$ .

### B. Grid map initialization

We used a grid map of a specified size and resolution to represent the environment. GPS coordinates  $\mathbf{g}_i$ , from the fingerprint vector, within the area bounded by each grid are grouped. This is achieved by referencing the origin of the grid map from a predetermined GPS coordinate and applying the transformation on the respective geographical location  $\mathbf{g}_i$  using GeographicLib [13] to each grid. The respective LTE data for these GPS coordinates are merged and each cell IDs will have an average RSS value. The collated LTE data are assigned to each grid which is referenced from its center in Cartesian coordinates with respect to the grid map. Hence, LTE data are mapped to the local grid map enabling localization in Cartesian coordinates. The corresponding LTE data from each GPS coordinates are associated with its grid and forms the fingerprint map in equation 2.

$$\mathbf{m} = \{(\mathbf{f}_1, \mathbf{h}_1), \dots, (\mathbf{f}_M, \mathbf{h}_M)\} \quad (2)$$

for a grid map  $\mathbf{m}$  with  $M$  re-associated fingerprints where  $\mathbf{f}_i$  is the LTE data associated with grid coordinates  $\mathbf{h}_i$ .

#### IV. LOCALIZATION

##### A. KNN-based localization

For LTE localization, LTE receivers actively scan and receive LTE data which is checked against the fingerprint map. In order to estimate the position of a mobile robot, we used KNN between the current received LTE data and the fingerprint map. We compute the cosine similarities, as shown in equation 3, between the current received LTE data and those that are stored in the fingerprint map. The similarities are sorted in descending order and the top  $K$  positions from the fingerprint map were selected. We obtain the estimated position as the weighted mean of the  $K$  coordinates in equation 4.

$$\text{sim}(\mathbf{z}, \mathbf{f}) = \frac{\sum_{l=1}^L \mathbf{f}_l \mathbf{z}_l}{\sqrt{\sum_{l=1}^L \mathbf{f}_l^2} \sqrt{\sum_{l=1}^L \mathbf{z}_l^2}} \quad (3)$$

where similarity of 0 indicates total dissimilarity and 1 indicates total similarity.

$$\hat{\mathbf{x}}_t = \frac{1}{\sum_{j=1}^K \text{sim}(\mathbf{z}_t, \mathbf{f}_{\pi(j)})} \sum_{j=1}^K \mathbf{x}_{\pi(j)} \cdot \text{sim}(\mathbf{z}_t, \mathbf{f}_{\pi(j)}) \quad (4)$$

##### B. Particle filter implementation

Particle filter based localization method is widely known and applied in mobile robot localization [14] [15]. The advantage of using particle filters is the ability to model non-parametric multi-modal distributions. Hence, it is ideal for non-linear applications as it allows for state estimation without prior knowledge or assumption of the state distribution [16]. The particle filter is able to model these distributions through ‘particles’ which are instances that are sampled from a stochastic process.

The system is represented by a state-space model where we want to estimate the position of a mobile robot given the applied changes in odometry and received LTE data for localization. We used Recursive Bayesian estimation for modelling the position estimation process of the system, which is shown in equation 5. The particle filter is used for its implementation and represents the belief of the robot’s position by a set of  $N$  weighted particles. This consists of three steps that iteratively optimises the path of the robot which are the prediction step, the update step and conditional resampling.

$$\begin{aligned} p(\mathbf{x}_t | \mathbf{z}_{1:t}, \mathbf{u}_{1:t}, \mathbf{m}) &= \eta_t \cdot p(\mathbf{x}_t | \mathbf{x}_{t-1}, \mathbf{u}_t) \\ &\cdot p(\mathbf{z}_t | \mathbf{x}_t, \mathbf{m}) \\ &\cdot p(\mathbf{x}_{t-1} | \mathbf{z}_{1:t-1}, \mathbf{u}_{1:t-1}, \mathbf{m}) \end{aligned} \quad (5)$$

The position,  $\mathbf{x}_t$  at time  $t$ , is estimated given the measurements,  $\mathbf{z}_{1:t}$ , control inputs,  $\mathbf{u}_{1:t}$ , and fingerprint map,  $\mathbf{m}$ , by the motion model  $p(\mathbf{x}_t | \mathbf{x}_{t-1}, \mathbf{u}_t)$  and observation model  $p(\mathbf{z}_t | \mathbf{x}_t, \mathbf{m})$ .  $\eta_t$  is the normalizer which ensures that the total probability is equals to one.

1) *Prediction step:* The motion model  $p(\mathbf{x}_t | \mathbf{x}_{t-1}, \mathbf{u}_t)$ , represents the likelihood of the position estimate  $\mathbf{x}_t$  at time  $t$  when control input  $\mathbf{u}_t$  is applied to the prior position estimate  $\mathbf{x}_{t-1}$ . The prediction of the posterior position is shown in equation 6 and 7. We obtain the changes in position,  $\Delta d_t$  through odometry from the robot.

$$x_t = x_{t-1} + \Delta d_t \cdot \cos(\theta_{t-1}) \cdot (1 + N(0, \sigma_d^2)) \quad (6)$$

$$y_t = y_{t-1} + \Delta d_t \cdot \sin(\theta_{t-1}) \cdot (1 + N(0, \sigma_d^2)) \quad (7)$$

Where  $\sigma_d^2$  is the Gaussian noise added to the change in displacement.

2) *Update step:* The observation model  $p(\mathbf{z}_t | \mathbf{x}_t, \mathbf{m})$ , represents the likelihood of obtaining the LTE measurement  $\mathbf{z}_t$  at the predicted posterior position  $\mathbf{x}_t$  given a fingerprint map  $\mathbf{m}$ . This is achieved by using KNN-based localization to update the weights of the particles in the particle filter. By comparing the measurement  $\mathbf{z}_t$  with the fingerprint map  $\mathbf{m}$ , we obtain the top  $K$  positions based on descending order of similarity, computed using the cosine similarity in equation 3.  $p(\mathbf{z}_t | \mathbf{x}_t, \mathbf{m})$  is estimated based on the distance measured between  $\mathbf{x}_t$  and  $\mathbf{h}_{\pi(j)}$  from the  $K$  coordinates obtained from the map in equation 8.

$$p(\mathbf{z}_t | \mathbf{x}_t, \mathbf{m}) \approx \sum_{j=1}^K \text{sim}(\mathbf{z}_t, \mathbf{f}_{\pi(j)}) \exp\left(-\frac{1}{2} d^2(\mathbf{x}_t, \mathbf{h}_{\pi(j)})\right) \quad (8)$$

where  $d^2(\cdot)$  is the squared distance measure as described in 9.

$$d^2(\mathbf{x}_t, \mathbf{h}_{\pi(j)}) = \frac{(x_t - x_{\pi(j)})^2}{\lambda} + \frac{(y_t - y_{\pi(j)})^2}{\lambda} \quad (9)$$

where  $\lambda$  is the variance of the displacement between  $\mathbf{x}_t$  and  $\mathbf{h}$

3) *Conditional resampling:* Particles are resampled through Sampling Importance Resampling (SIR) which removes ‘particles’ that are less likely to represent the current position of the robot accurately. Resampling prevents the sample degeneracy problem in particle filters but, it would cause the sample impoverishment problem if it is done constantly for every time step [17]. Hence, to address this issue, a threshold is set using Effective Sample Size, in equation 10 as the condition for when resampling has to be done [18]. The particle filter method is described as a block diagram in figure 2.

$$\widehat{ESS} = \frac{1}{\sum_{n=1}^N \bar{w}_n^2} \quad (10)$$

where  $\bar{w}_n$  is the normalized importance weights.

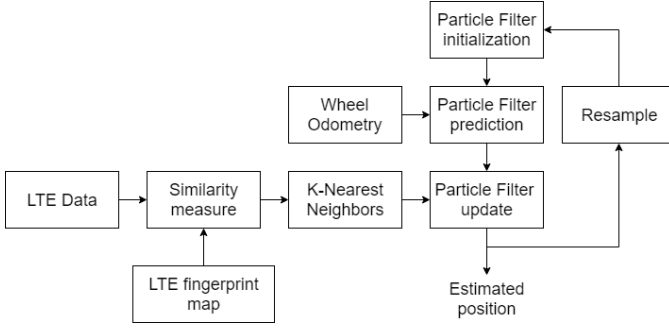


Fig. 2. This figure shows the block diagram of the particle filter method.

## V. EXPERIMENTAL RESULT

### A. Setup

A 500m x 500m map with a grid resolution of 5m was initialized. The LTE fingerprint map was built using LTE data from five different cellular bands from two local cellular networks, Singtel and M1 together with its corresponding GPS coordinates. This was collected using five Xiaomi Mi Max 3 smartphones running an app created to scan and record the required data while moving all around the campus of Singapore University of Technology and Design as shown in figure 3. A total of 757 locations were sampled for fingerprints.

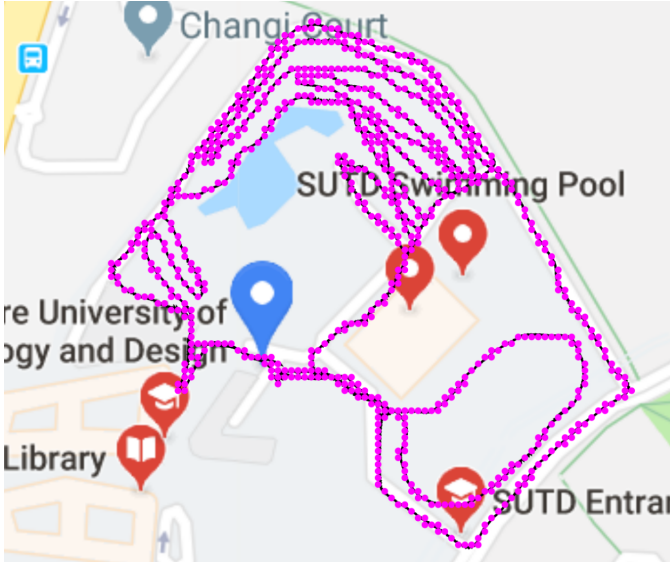


Fig. 3. This figure shows the path taken to obtain the fingerprints. The pink dots are the fingerprint sampling locations.

The experiment is performed on Clearpath Robotics Husky Unmanned Ground Vehicle (UGV) which uses a skid-steer drive. A Jetson TX2 running the Robot Operating System (ROS) was used to control the Husky UGV and to obtain its wheel odometry. GPS and LTE data from five different cellular

bands are obtained from five Xiaomi Mi Max 3 smartphones, at 0.5Hz, which are placed on the Husky UGV as shown in figure 4. In each scan, each smartphone receives at least two sets of cell ID and mean RSS from its respective band. The GPS data is taken to be the ground truth in this experiment.

The experiment was conducted on the roads within Singapore University of Technology and Design. The terrain of the roads has upward and downward slopes, bumps, shelters and runs through buildings and open fields. The Husky UGV was driven a total of 6 rounds, 4 rounds in the anticlockwise direction and 2 rounds in the clockwise direction, on the route described in figure 5. We obtained 232 LTE data scanning points and the robot had an average velocity of 1m/s and travelled a total distance of approximately 4920m (approximately 820m per round).

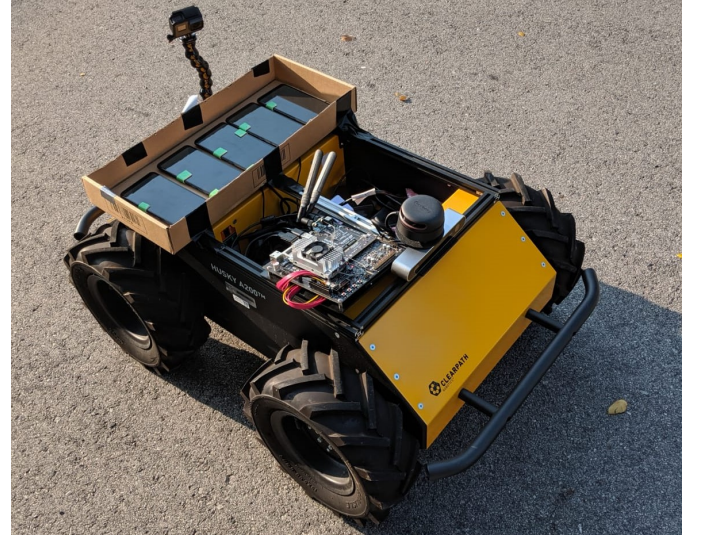


Fig. 4. This figure shows the setup of the robot used for the experiment

The particle filter was initialized with 1000 particles and  $\lambda$  was set to 30. The Gaussian noises  $\sigma_d$  and  $\sigma_\theta$  was set to 10m and 0.5rad respectively.

### B. Localization accuracy

From the experiment, the Root Mean Square Error (RMSE) of each method was computed and describes its accuracy. The particle filter obtained a low RMSE of 13.07m, which is superior as compared to using wheel odometry, RMSE of 75.13m, and KNN localization, RMSE of 35.20m, as shown in table I. Figure 6 shows that the particle filter was outperforming both wheel odometry and KNN-based localization.

TABLE I  
RMSE OF LOCALIZATION METHODS

	Wheel odometry	KNN localization	PF localization
RMSE (m)	75.13	35.20	13.07

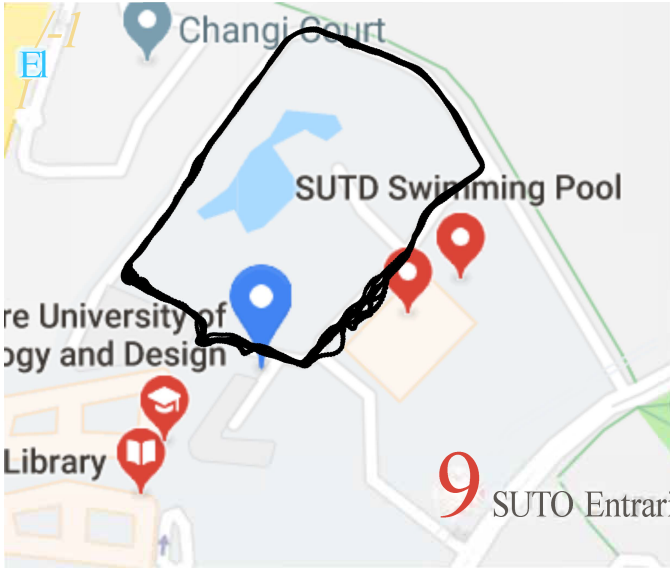


Fig. 5. This figure shows the route travelled for the experiment.

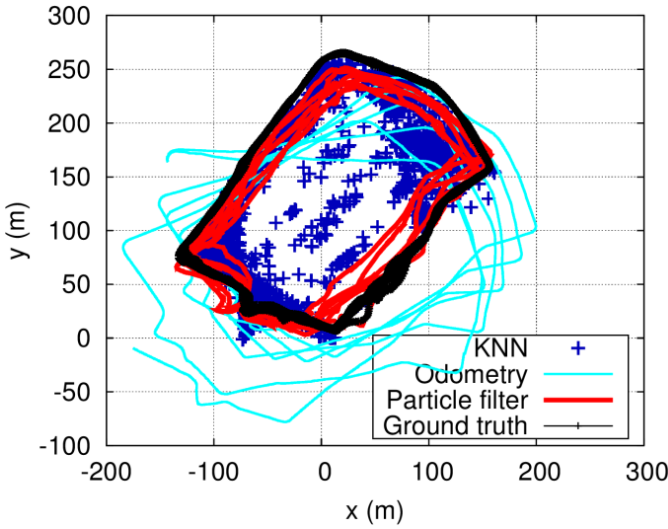


Fig. 6. This figure shows the trajectories of the respective localization methods including ground truth.

### C. Parameter effects on the localization method

We evaluate the parameters of the localization method to study its effects on the localization accuracy. The parameters include number of LTE bands that was used in fingerprinting and localization, the  $K$  value of KNN, the particle size of the particle filter, the grid resolution of the grid map, the Gaussian noises,  $\sigma_d$  and  $\sigma_\theta$ , of the wheel odometry and the  $\lambda$  value in equation 9. We obtain a RMSE of 13.07m for the localization method using the optimal values of each parameter.

1) *LTE bands*: The KNN-based localization had the best result when LTE data from 4 different cellular bands were obtained while PF-based localization had the best results with 5 bands. This can be seen in table II where the RMSE decreases with increasing number of cellular bands. With

increasing cellular bands, both the fingerprint map and LTE data obtained from the experiment uses more information for localization. Hence, improving the localization accuracy of the method.

TABLE II  
INCREMENTAL USE OF BANDS ON LOCALIZATION ACCURACY

Band	RMSE (m) KNN	RMSE (m) PF
Singtel B7	61.06	45.89
+ Singtel B8 (2 bands)	40.74	18.89
+ Singtel B3 (3 bands)	37.11	18.24
+ M1 B7 (4 bands)	34.90	16.32
+ M1 B3 (5 bands)	35.20	13.07

2) *K value in KNN*: Choosing the top  $K$  fingerprints allow for approximation of the system by choosing those top most significant particles to represent the system. When tuning parameter  $K$ , a larger value would increase the amount of data for computing the weighted mean of the  $K$  coordinates. Hence, this would increase the uncertainty of the position estimation. This can be seen in table III where the most optimal value of  $K$  for localization accuracy is 4 which has the lowest RMSE of 35.20m and 17.29m for KNN and PF respectively.

TABLE III  
RMSE OF KNN LOCALIZATION USING DIFFERENT NUMBER OF  $K$

$K$ value	1	4	8	16	32	64
RMSE (m) KNN	37.34	35.20	35.72	37.41	40.14	43.82
RMSE (m) PF	16.87	13.07	13.78	15.94	18.06	19.05

3) *Particle size*: Particle size describes the ability of the particle filter to model a distribution accurately. Larger particle size indicates better representation of the distribution of the system. However, computation load scales with particle size as more calculations are performed for the particles. In table IV, we obtain the optimal particle size to be 1000 with the lowest RMSE of 13.07m and acceptable average running time of 0.0254s.

TABLE IV  
PARTICLE SIZE ON LOCALIZATION ACCURACY AND AVERAGE RUNNING TIME

Particles	10	100	500	1000	2000	5000
RMSE (m)	36.81	13.31	13.43	13.07	13.61	13.09
Time (s)	0.0225	0.0228	0.0234	0.0254	0.0261	0.0303

4) *Grid resolution*: Grid resolution affects the association of LTE data with grid map coordinates. Increasing grid resolution reduces the association of LTE data as there are lesser coordinates and thus, affects the accuracy of estimating the position of the robot. However, higher grid resolution would reduce computational load as there are lesser similarities to compute when checking the LTE data against the fingerprint



map. Table V shows that a grid resolution of 5m and 20m produces the best localization accuracy for PF-based localization and KNN-based localization respectively. A grid resolution of 80m gives fastest average running time.

TABLE V  
GRID RESOLUTION ON LOCALIZATION ACCURACY AND AVERAGE RUNNING TIME

Grid Resolution (m)	2.5	5	10	20	40	80
RMSE (m) KNN	39.74	35.20	34.76	34.37	43.89	63.67
RMSE (m) PF	16.26	13.07	16.14	18.67	30.82	43.06
Time (s)	0.0586	0.0254	0.0127	0.0074	0.0058	0.0055

5) *Gaussian noises,  $\sigma_d$  and  $\sigma_\theta$ , and  $\lambda$  value:* We tune the process noise of the system to obtain the best localization result. Based on figure 7, we obtained the lowest mean localization error for when  $\sigma_d$  is 1 and  $\sigma_\theta$  is 0.1. A lambda of 30 also yields a lower RMSE of 13.07m as shown in table VI.

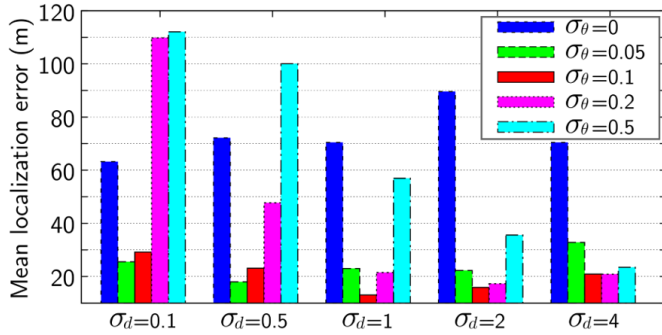


Fig. 7. This figure shows the mean localization error based on the different combination of  $\sigma_d$  and  $\sigma_\theta$  Gaussian noise values

TABLE VI  
 $\lambda$  VALUE ON LOCALIZATION ACCURACY

$\lambda$	10	20	30	40	80	100	200
RMSE (m)	19.15	14.33	13.07	13.97	14.41	14.95	17.13

## VI. CONCLUSIONS

This paper has proposed a low-cost mobile robot outdoor localization method using a particle filter based localization method which only uses LTE with KNN and wheel odometry. In GPS denied outdoor environments, the particle filter based LTE localization proves to be an accurate alternative method for localization with RMSE of 13.07m as compared to LTE localization using KNN or wheel odometry localization. This especially benefits mobile robots that do not have an array of sensors to rely on for SLAM and localization or constrained by cost, weight and size. It is worth noting that the method did not require any additional infrastructure since it makes use of existing ones. Hence, mobile robots that are designed for outdoor environments should consider LTE as one of its localization methods to ensure consistency in accurate

localization results when maneuvering in locations that do not always provide a GPS fix. Additionally, this method could be extended to any robotic platforms that are able to obtain positional information and LTE data.

## REFERENCES

- [1] Bailey, T. (2002). Mobile robot localisation and mapping in extensive outdoor environments. Australian Centre for Field Robotics, Department of Aerospace, Mechanical and Mechatronic Engineering, University of Sydney.
- [2] Emter, T., Petereit, J. (2014, May). Integrated multi-sensor fusion for mapping and localization in outdoor environments for mobile robots. In Multisensor, Multisource Information Fusion: Architectures, Algorithms, and Applications 2014 (Vol. 9121, p. 912100). International Society for Optics and Photonics.
- [3] Liu, R., Yuen, C., Do, T. N., Zhang, M., Guan, Y. L., Tan, U. X. (2019). Cooperative positioning for emergency responders using self IMU and peer-to-peer radios measurements. Information Fusion.
- [4] Brand, C., Schuster, M. J., Hirschmüller, H., Suppa, M. (2014, September). Stereo-vision based obstacle mapping for indoor/outdoor SLAM. In 2014 IEEE/RSJ International Conference on Intelligent Robots and Systems (pp. 1846-1853). IEEE.
- [5] Balasuriya, B. L. E. A., Chathuranga, B. A. H., Jayasundara, B. H. M. D., Napagoda, N. R. A. C., Kumarawadu, S. P., Chandima, D. P., Jayasekara, A. G. B. P. (2016, April). Outdoor robot navigation using Gmapping based SLAM algorithm. In 2016 Moratuwa Engineering Research Conference (MERCon) (pp. 403-408). IEEE.
- [6] Gu, Y., Wada, Y., Hsu, L., Kamijo, S. (2014, November). Vehicle self-localization in urban canyon using 3D map based GPS positioning and vehicle sensors. In 2014 International Conference on Connected Vehicles and Expo (ICCVE) (pp. 792-798). IEEE.
- [7] Yassin, A., Nasser, Y., Awad, M., Al-Dubai, A., Liu, R., Yuen, C., ... Aboutanios, E. (2016). Recent advances in indoor localization: A survey on theoretical approaches and applications. IEEE Communications Surveys Tutorials, 19(2), 1327-1346.
- [8] Liu, R., Yuen, C., Do, T. N., Tan, U. X. (2017). Fusing similarity-based sequence and dead reckoning for indoor positioning without training. IEEE Sensors Journal, 17(13), 4197-4207.
- [9] Kos, T., Markezic, I., Pokrajacic, J. (2010, September). Effects of multipath reception on GPS positioning performance. In Proceedings ELMAR-2010 (pp. 399-402). IEEE.
- [10] Mirowski, P., Ho, T. K., Yi, S., MacDonald, M. (2013, October). SignalSLAM: Simultaneous localization and mapping with mixed WiFi, Bluetooth, LTE and magnetic signals. In International Conference on Indoor Positioning and Indoor Navigation (pp. 1-10). IEEE.
- [11] Ye, X., Yin, X., Cai, X., Yuste, A. P., Xu, H. (2017). Neural-network-assisted UE localization using radio-channel fingerprints in LTE networks. Ieee Access, 5, 12071-12087.
- [12] Abdallah, A. A., Saab, S. S., Kassas, Z. M. (2018). A machine learning approach for localization in cellular environments. 2018 IEEE/ION Position, Location and Navigation Symposium (PLANS). doi:10.1109/plans.2018.8373508
- [13] C. F. Karney, GeographicLib, Version 1.49 (2017-10-05), <https://geographiclib.sourceforge.io/1.49>
- [14] Ganganath, N., Leung, H. (2012, January). Mobile robot localization using odometry and kinect sensor. In 2012 IEEE International Conference on Emerging Signal Processing Applications (pp. 91-94). IEEE.
- [15] Röwekämper, J., Sprunk, C., Tipaldi, G. D., Stachniss, C., Pfaff, P., Burgard, W. (2012, October). On the position accuracy of mobile robot localization based on particle filters combined with scan matching. In 2012 IEEE/RSJ International Conference on Intelligent Robots and Systems (pp. 3158-3164). IEEE.
- [16] Havangi, R., Nekoui, M. A., Teshnehlab, M. (2010). A multi swarm particle filter for mobile robot localization. International Journal of Computer Science, 7(3), 15-22.
- [17] Li, T., Sun, S., Sattar, T. P., Corchado, J. M. (2014). Fight sample degeneracy and impoverishment in particle filters: A review of intelligent approaches. Expert Systems with applications, 41(8), 3944-3954.
- [18] Martino, L., Elvira, V., Louzada, F. (2017). Effective sample size for importance sampling based on discrepancy measures. Signal Processing, 131, 386-401.